

## SOOT FORMATION AT ELEVATED PRESSURES AND CARBON CONCENTRATIONS IN HYDROCARBON PYROLYSIS

ST. BAUERLE, Y. KARASEVICH, ST. SLAVOV, D. TANKE, M. TAPPE, TH. THIENEL AND H. GG. WAGNER

*University of Göttingen  
Tammanstrasse 6, Göttingen 37077, Germany*

For the formation of soot in mixtures of ethylene, *n*-hexane, and benzene in argon behind reflected shock-wave induction periods, soot growth rate constants and soot yields were measured at various temperatures, pressures, and C-atom concentrations using light extinction techniques.

As expected, the three substances investigated behave differently regarding soot formation, the strongest difference being between aromatic and nonaromatic fuels. Induction times and soot growth rate constants do not show any significant pressure effect within the accuracy of the experiment under the conditions employed. The data for ethylene and *n*-hexane agree quantitatively fairly well, whereas benzene shows induction times that are shorter and rate constants that are larger by about an order of magnitude than those of the nonaromatics for equal C-atom concentrations.

The previously observed general shape and behaviour of the soot yield curves could be confirmed, with maximum soot yields, at temperatures between 1800 and 1950 K. For similar experimental conditions of temperature, pressure, and carbon concentration, the sooting propensity increases from *n*-hexane to ethylene to benzene. The large pressure range covered in this study revealed different pressure dependencies of soot formation for the three hydrocarbons investigated. For *n*-hexane, the influence of pressure on soot yield in pyrolysis is very small. For ethylene, soot yield scales with pressure, whereas for benzene, a different behaviour was found, resulting in lower soot yields at higher pressures at otherwise equal conditions. Soot yields are also depending on C-atom concentration. Particle diameters of soot from pyrolysis determined by electron microscopy can be described by a narrow log-normal size distribution, with  $\sigma_g \approx 0.2$ . The average particle diameters are 20–30 nm for all conditions of temperature, pressure, and C-atom concentration employed in this study. Assuming spherical particles, this leads to final number densities of  $10^{11}$  to  $10^{13}/\text{cm}^3$ .

### Introduction

In practical combustion devices, soot formation and oxidation depend on fuel type, mixture composition, pressure, and temperature (for reviews, see e.g. Refs. 1 through 5). One of the important technical parameters is the pressure at which combustion takes place. While stationary burners mostly operate close to atmospheric pressure, values above 100 bar may be reached in modern diesel engines. The shock-tube technique allows one to study soot formation under controlled conditions, at temperatures, pressures, and carbon concentrations similar to those in practical applications.

For a number of unsaturated hydrocarbons pyrolysis experiments in shock tubes have been performed below 10 bar [6–9]. These experiments show a rather typical dependence of soot formation on temperature, carbon density, and fuel structure. At higher pressures up to 250 bar, rates of soot formation in shock tubes have been measured at temperatures between 1700 and 2800 K for ethylene [10]. High-pressure shock-tube experiments on the pyrolysis of *n*-hexane have been performed by Hwang et al. [11].

Here, experiments are described about soot formation under similar pyrolytic conditions with ethylene, *n*-hexane, and benzene, performed behind reflected shock waves at temperatures between 1700 and 2300 K for pressures up to 100 bar and C-atom concentrations between  $2 \cdot 10^{17}$  and  $2 \cdot 10^{19}$  C atoms/ $\text{cm}^3$ . The measurements were especially performed in order to determine the influence of pressure on soot formation and separate it from that of C-atom density.

Three different techniques have been used: (1) extinction measurements of a HeNe laser beam at 632.8 nm, (2) gas chromatography (GC) analysis of gaseous end products, and (3) analysis of soot samples by electron microscopy.

Quantities to characterize soot formation are the induction period of soot formation  $\tau$ , the soot yield SY, the formal soot growth rate  $k_f$ , final particle diameters and number densities as functions of temperature, C-atom concentration, fuel structure, and especially pressure.

### Experimental

The experimental setup has been described previously [11]; therefore, only a few details are given.

The experiments were performed behind reflected shock waves in a 70-mm i.d. steel shock tube with a 4.5-m-long driven section, a 3.5-m-long driver section, and a 28-mm-thick tube wall. Shock speed was measured with Kistler piezoelectric pressure transducers. Reflected shock parameters were calculated [12,13] using the measured incident shock speed. The typical shock wave attenuation was always less than 2%/m.

The conversion of hydrocarbon to soot was measured via the attenuation of the light beam from a 15-mW HeNe laser operated at  $\lambda = 632.8$  nm. The light extinction profiles  $I(t)$  were converted into soot volume fraction profiles  $f_v(t)$  using Beer's law [6] and the refractive index given by Lee and Tien [14]. A sampling flask [15] allowed the taking of gas and soot samples simultaneously. The valve opened at about 5 ms after the reflected shock wave passed for about 10 ms. Directly afterwards, the gas samples were gas chromatographically analyzed on a GC (Packard Model 419) with 5-ft 60/80 mesh Carbosieve and 2-m 5 Å molecularsieve columns. The following substances were quantitatively determined:  $H_2$ ,  $CH_4$ ,  $C_2H_2$ ,  $C_2H_4$ , and  $C_2H_6$ . Soot was collected on carbon film grids (mesh size 400) and on Al surfaces. Soot particle diameters were determined with transmission electron microscope (TEM) and raster electron microscope (REM).

The hydrocarbon/argon test gas mixtures were prepared manometrically and mixed by convection in stainless steel cylinders at least 48 h before use. The gases ethylene (>99.8% Linde) and Ar (>99.998% Messer-Griesheim) were used without further purification. Benzene (>99.7% Riedel-De Haen) and *n*-hexane (>97% Merck) were purified by distillation. Total densities behind reflected shock waves were varied from  $3 \cdot 10^{-5}$  to  $70 \cdot 10^{-5}$  mol/cm<sup>3</sup>, C-atom concentrations were varied from  $2 \cdot 10^{17}$  to  $2 \cdot 10^{19}$  atoms/cm<sup>3</sup> in the temperature range 1700–2300 K.

## Experimental Results

Figure 1 shows a typical soot concentration time profile for benzene pyrolysis together with the measured pressure. Clearly visible are the passage of the incident and reflected shock front. After a short induction period, the soot concentration increases strongly and tends towards a constant value that determines soot yield SY.

The absolute value of the induction period  $\tau$  depends somewhat on the experimental technique used. However, the order of magnitude and the dependence on parameters like pressure, temperature, and C-atom concentration should be similar for different experimental techniques. Here, the induction time  $\tau$  is defined as the intersection of the inflectional tangent with the time axis, as indicated in Fig. 1.

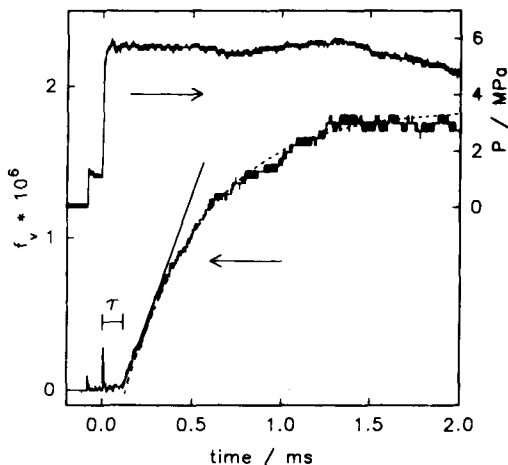


FIG. 1. Converted soot concentration profile and experimental pressure record for benzene pyrolysis:  $T = 1890$  K,  $P = 50$  bar,  $[C] = 5 \cdot 10^{17}$ /cm<sup>3</sup>. Upper line: Pressure time profile; lower line: soot concentration time profile; dashed line: first-order fit ( $k_f = 2200$  s<sup>-1</sup>,  $f_{v\infty} = 1.85 \cdot 10^{-6}$ ). In both signals, the incident and reflected waves are clearly visible. The expansion wave arrives after about 1.7 ms. The induction time  $\tau$  is defined as the intersection of the inflectional tangent with the time axis.

The plot shows the “smooth” start of soot formation that passes over into a fast growth region and slows down later on to reach a constant value of  $f_v$ , the final soot volume fraction  $f_{v\infty}$ .

The upper parts of the  $f_v$  profiles are approximated by an empirically obtained first-order rate law [10,16], where  $k_f$  is used as a measure for the rate of soot formation:

$$\frac{df_v}{dt} = k_f \cdot (f_{v\infty} - f_v). \quad (1)$$

The dashed line in Fig. 1 shows how the apparent first-order rate constant of soot mass growth  $k_f$  and the final soot volume fraction  $f_{v\infty}$  were derived by a numerical fitting procedure. From the latter, soot yields were computed.

In general, the three substances investigated behave differently regarding soot formation under pyrolytic conditions. This will be discussed in the following for  $\tau$ ,  $k_f$ , average particle diameters  $d_{\infty}$ , and SY.

### Induction Time:

The influence of temperature, pressure, and C-atom concentration on the induction period  $\tau$  was investigated. Figure 2 shows the influence of temperature for a fixed carbon density in an Arrhenius-type diagram. Plotted is  $\log(1/\tau)$  vs  $1/T$  for benzene

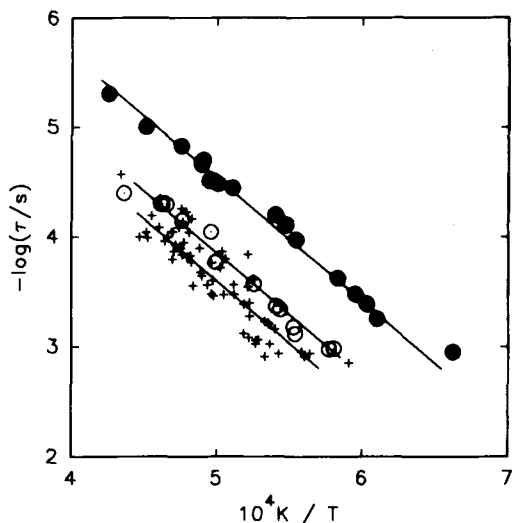


FIG. 2. Arrhenius-type plot of  $\log(1/\tau)$  vs.  $1/T$  for the three hydrocarbons investigated.  $\bullet$ : benzene,  $P = 50$  bar,  $[C] = 2.5 \cdot 10^{18}/\text{cm}^3$ ;  $\circ$ : ethylene,  $P = 50$  bar,  $[C] = 2.5 \cdot 10^{18}/\text{cm}^3$ ;  $+$ :  $n$ -hexane,  $P = 20$ – $100$  bar,  $[C] = 3.2 \cdot 10^{18}/\text{cm}^3$ ; solid lines: best fits.

( $p = 50$  bar,  $[C] = 2.5 \cdot 10^{18}/\text{cm}^3$ ), ethylene ( $p = 50$  bar,  $[C] = 2.5 \cdot 10^{18}/\text{cm}^3$ ), and  $n$ -hexane ( $p = 25$ – $100$  bar,  $[C] = 3.2 \cdot 10^{18}/\text{cm}^3$ ). For the three hydrocarbons investigated, linear curves with similar activation energies of about  $215$  kJ/mol but different pre-exponential factors are obtained. As the curve for hexane shows, under the conditions employed, practically no pressure dependence of the induction period is observed, in agreement with earlier experiments [11]. The same holds for ethylene and benzene. Figure 2 shows that as temperature increases,  $\tau$  decreases. For a given temperature and C-atom concentration, the beginning of soot formation for benzene pyrolysis is about an order of magnitude faster than for ethylene and hexane pyrolysis.

In general, as the C-atom concentration increases, the induction period decreases. For benzene, the C-atom concentration has been varied by two orders of magnitude, between  $2$  and  $250 \cdot 10^{17}$  C atoms/ $\text{cm}^3$ , and a strong dependence on carbon concentration is observed. The data fall onto one curve if normalized by C-atom concentration. The curve can be expressed by

$$1/\tau = [C]^n \cdot A \cdot \exp(-E_{\text{ind}}/RT). \quad (2)$$

For benzene, the following parameters are obtained for carbon densities between  $0.4$  and  $40 \cdot 10^{-6}$  mol/ $\text{cm}^3$ :  $n = 0.75$ ,  $A = 3.2 \cdot 10^{15}$  ( $\text{cm}^3/\text{mol}$ ) $^{0.75}$  s $^{-1}$ , and  $E_{\text{ind}} = 260$  kJ/mol. Induction times from the benzene experiments of Graham [6] fit fairly well in this representation.

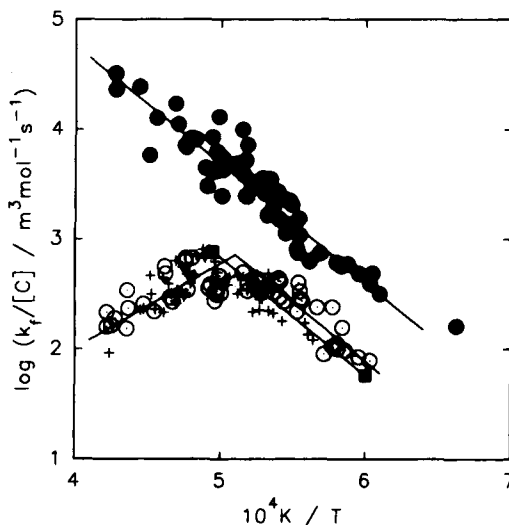


FIG. 3. Temperature dependence of the first-order rate  $k_f$ , normalized by the carbon concentration for the three hydrocarbons investigated.  $\bullet$ : benzene,  $P = 5$ – $50$  bar,  $[C] = 2.5$  to  $25 \cdot 10^{17}/\text{cm}^3$ ;  $\circ$ : ethylene,  $P = 6$ – $100$  bar,  $[C] = 2.0$  to  $6 \cdot 10^{18}/\text{cm}^3$ ;  $+$ :  $n$ -hexane,  $P = 25$ – $100$  bar,  $[C] = 3.2 \cdot 10^{18}/\text{cm}^3$ ;  $\blacksquare$ :  $10$  bar  $\text{C}_2\text{H}_4/\text{air}$  flame [21].

For ethylene C-atom concentrations of  $3$ – $14 \cdot 10^{-6}$  mol/ $\text{cm}^3$  were employed, and only a weak dependence is observed. For hexane, carbon densities were varied between  $5$  and  $40 \cdot 10^{-6}$  mol/ $\text{cm}^3$ , and hardly any dependence of  $\tau$  on C-atom concentration was found.

#### First-Order Rate Constant:

As described above, apparent first-order rate constants  $k_f$  were derived from the latter part of the experimental  $f_v$  curves by a fitting procedure. In this context,  $k_f$  has been interpreted [16,18–20] as an effective measure of the “active lifetime” of soot particles, assuming that they are losing their reactivity. The influence of temperature on  $k_f$  is shown in Fig. 3 in the form of an Arrhenius diagram. The rate constants can be rather well represented when they are normalized by the carbon concentrations. The pressure was varied between  $5$  and  $100$  bar, and no influence of pressure was observed on  $k_f/[C]$  for the three hydrocarbons investigated for the temperatures and carbon-atom concentrations employed in this study. For ethylene and  $n$ -hexane, the data can be represented by a single curve showing a maximum at a temperature of about  $2000$  K. For benzene, no maximum is observed in the temperature range covered. For a given temperature  $\leq 2000$  K and C-atom concentration, benzene has an up to  $10$  times higher rate constant  $k_f$  than ethylene and  $n$ -hexane. The apparent activation energies for the three hydrocarbons for

the temperature range 1600–2000 K again are very similar, with a value for  $E_{kf}$  of about 200 kJ/mol. Data from 10-bar ethylene/air premixed flames [21], normalized by an "effective" carbon concentration (discussed below), are also shown for this temperature range, and they are very similar to the ethylene/*n*-hexane shock-tube pyrolysis data.

#### Particle Size REM/TEM:

Soot samples were obtained from *n*-hexane and benzene pyrolysis. Samples were taken under all conditions employed in the optical measurements, at temperatures between 1700 and 2300 K, pressures between 25 and 100 bar, and C-atom concentrations in the range from 2 to  $200 \cdot 10^{17}/\text{cm}^3$ . The soot probes collected were examined by means of REM and TEM. The primary particles, approximated as spheres, are arranged in agglomerates. Only the diameters of clearly identifiable particles are determined. The results from REM (where the gold coating has to be taken into account) and TEM electron microscopy agree fairly well. The visual impression of the micrographs obtained from different experiments is identical. The diameters of primary spherical particles can be described by a log-normal size distribution with a geometric standard deviation  $\sigma_g$  of approximately 0.2. The way the soot samples were taken may slightly influence the size distribution present in the shock tube. The evaluations show that average soot particle diameters are in the range of 20–30 nm. These data indicate that in shock-tube pyrolysis, under the conditions applied here, C-atom concentration and pressure do not exhibit a marked influence on particle diameters.

#### Soot Yield:

Soot yield is defined as carbon present as soot referred to total carbon content. Carbon present as soot was calculated using the soot volume fraction  $f_{\text{soot}}$  [see Eq. (1)] and a soot density of  $\rho_{\text{soot}} = 1.86 \text{ g/cm}^3$ . In Fig. 4a, soot yield curves for ethylene, *n*-hexane, and benzene as a function of temperature for similar C-atom concentration and a pressure of  $P \approx 50$  bar are given. Additionally for *n*-hexane, the soot yield curves obtained at 25 and 100 bar coincide with the 50-bar soot yield curve. So, a single curve fits all *n*-hexane soot yield data. The soot yield curves show the bell shape observed by Graham et al. [6] and Frenklach et al. [8] for near-atmospheric pressure and by Hwang et al. [11] for high pressures. There is a pronounced maximum of soot yield with temperature, for ethylene near 1850 K, for *n*-hexane around 1950 K, and for benzene at about 1800 K. For a given C-atom concentration, benzene shows a much higher propensity to soot than ethylene and *n*-hexane. Only a slight dependence of the maximum

temperature  $T_{\text{SY,max}}$  on C-atom concentration is observed.

Gaseous end products of shock-tube pyrolysis were sampled and analyzed by GC. Measurements were made for various temperatures at a pressure of 50 bar for concentrations of 7.5 and  $200 \cdot 10^{17}$  C atoms/ $\text{cm}^3$  for benzene, and for ethylene and *n*-hexane at concentrations of  $35 \cdot 10^{17}$  C atoms/ $\text{cm}^3$ . Quantitatively analyzed were  $\text{H}_2$ ,  $\text{CH}_4$ ,  $\text{C}_2\text{H}_2$ ,  $\text{C}_2\text{H}_4$ , and  $\text{C}_2\text{H}_6$ . By the use of a reference substance in the shocked gas, concentrations could be determined with an accuracy of about 10%. Concentrations were measured absolutely, and yields were referred to the total carbon concentrations employed. The GC and optical measurements were independent of each other, but the mass balances for C and H atoms for the different experiments fit fairly well, confirming the refractive index used [14]. The main hydrocarbons found were  $\text{C}_2\text{H}_2$  and  $\text{CH}_4$ .

Quantitative yields of these gas products for a temperature of 1900 K and C-atom concentration of  $\approx 3 \cdot 10^{18}/\text{cm}^3$  were calculated. The final acetylene (methan) yield found was 45% (3%) for *n*-hexane pyrolysis, 40% (1%) for ethylene pyrolysis, and 30% (less than 1%) for benzene pyrolysis.

For the three hydrocarbons investigated, the  $\text{C}_2\text{H}_2$  concentrations show a pronounced minimum at the temperature where the soot yields exhibit a maximum. For benzene, e.g., at the maximum temperature  $T_{\text{SY,max}} = 1800$  K, about 20% of carbon was converted to gaseous end products. This is consistent with a soot yield of 80% found for this condition. In general, for the temperature region 1800–2300 K, the amount of carbon found in the gas phase as percentage of total carbon concentration is complementary to the soot yield curves, for all conditions employed.

The influence of pressure on soot yield is different for the three hydrocarbons investigated. Hardly any pressure dependence is observed for *n*-hexane at pressures between 20 and 100 bar. Only a slight shift of the curve towards higher temperatures for lower pressures can be noticed [11]. For ethylene, the soot yield data as a function of pressure and temperature for similar C-atom concentrations are plotted in Fig. 4b. There is an increase in soot yield from about 45% at 25 bar to 90% at 100 bar. The data show that ethylene soot yield SY is proportional to  $P_{\text{tot}}$ ; this trend holds down to pressures of about 6 bar [15]. Tanke [15] also reports a strong dependence of soot yield on C-atom concentration.

For benzene, data for pressures of 5 and 50 bar and different C-atom concentrations are shown in Fig. 4c. The curves represent best fits, and practically the same curve is found for the data symbolized by  $\times$  and  $\triangle$ . Data below 1700 K are not shown as induction periods become too long. The  $\times$  and  $\diamond$  denote soot yields for similar C-atom concentrations at pressures of 5 and 50 bar. The 5 bar data are taken

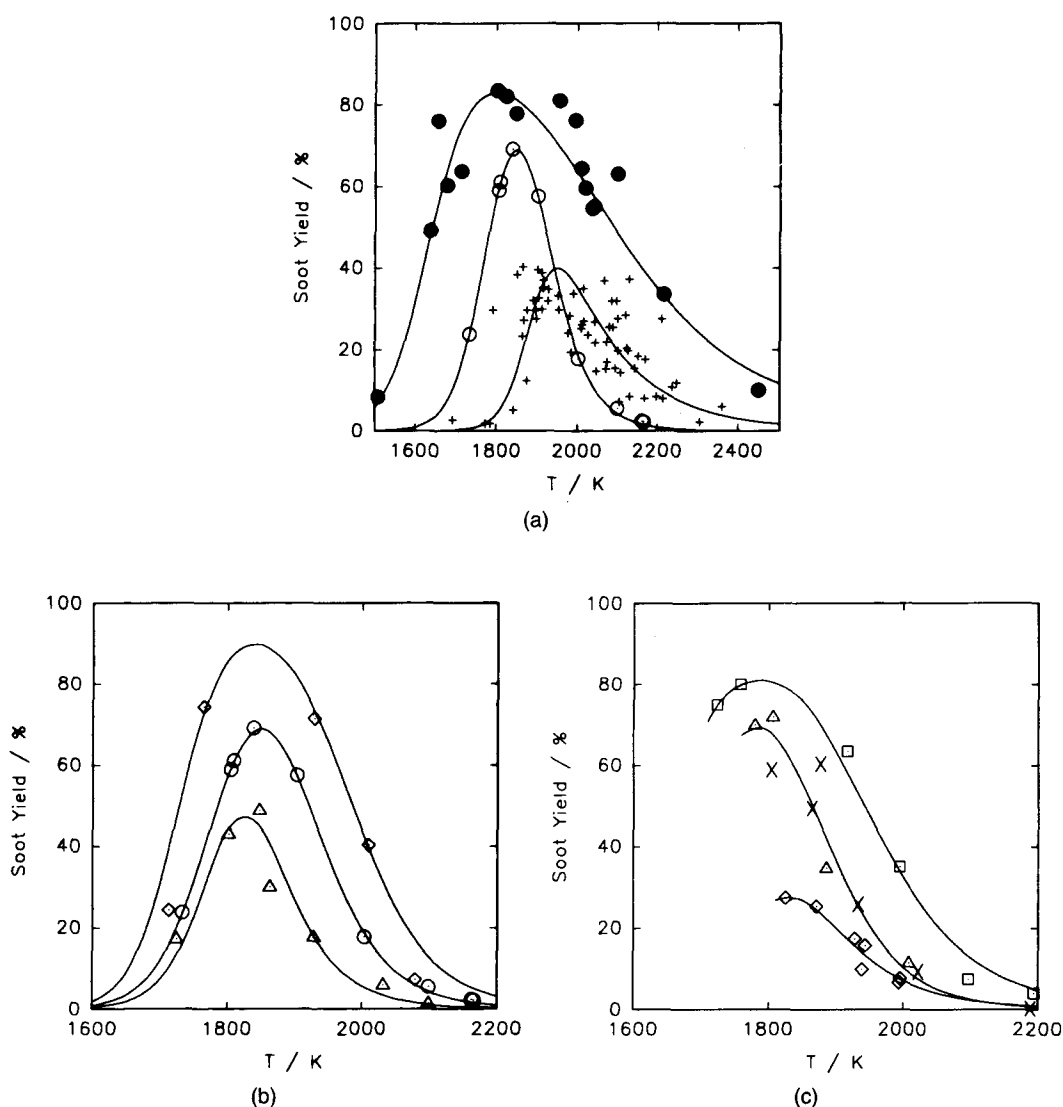


FIG. 4. (a) Plot of soot yield SY vs  $T$  for the three hydrocarbons investigated.  $\bullet$ : benzene,  $P = 50$  bar,  $[C] = 2.5 \cdot 10^{18} / \text{cm}^3$ ;  $\circ$ : ethylene,  $P = 50$  bar,  $[C] = 2.5 \cdot 10^{18} / \text{cm}^3$ ;  $+$ :  $n$ -hexane,  $P = 20$ – $100$  bar,  $[C] = 3.2 \cdot 10^{18} / \text{cm}^3$ ; solid lines: best fits. (b) Plot of soot yield SY vs  $T$  for ethylene pyrolysis at three different pressures, for a constant carbon concentration  $[C] = 2.5 \cdot 10^{18} / \text{cm}^3$ .  $\triangle$  triangle up:  $P = 25$  bar;  $\circ$ :  $P = 50$  bar;  $\diamond$ :  $P = 100$  bar; solid lines: best fits. (c) Plot of soot yield SY vs  $T$  for benzene pyrolysis at different pressures and carbon concentrations.  $\diamond$ :  $P = 50$  bar,  $[C] = 2.5 \cdot 10^{17} / \text{cm}^3$ ;  $\triangle$ :  $P = 50$  bar,  $[C] = 5.0 \cdot 10^{17} / \text{cm}^3$ ;  $\square$ :  $P = 50$  bar,  $[C] = 7.5 \cdot 10^{17} / \text{cm}^3$ ;  $\times$ :  $P = 5$  bar,  $[C] = 2.5 \cdot 10^{17} / \text{cm}^3$ ; solid lines: best fits.

under similar conditions as those of Graham et al. [6], and the observed dependence of soot yield with temperature is in accordance with his results. Furthermore, Fig. 4c shows a decrease in soot yield from low pressure (5 bar) to high pressure (50 bar) at equal carbon concentrations. This differs from the pressure dependence observed for ethylene.

The data represented by open symbols shows the

influence of carbon concentration. Soot yield curves for benzene pyrolysis at a pressure of 50 bar for benzene fractions of 200, 400, and 600 ppm are plotted, showing an increase in soot yield with increasing carbon concentration for a given temperature and pressure.

Combining all the data demonstrates the dependence of soot yield on pressure and C-atom concen-

tration. The soot yield indicated by the middle curve can be achieved either by a pressure of 5 bar and a carbon concentration of  $2.5 \cdot 10^{17}$  atoms/cm<sup>3</sup> ( $\times$ ) or by a pressure of 50 bar and a carbon concentration of  $5.0 \times 10^{17}$  atoms/cm<sup>3</sup> ( $\Delta$ ). For a given carbon concentration ( $2.5 \cdot 10^{17}$  atoms/cm<sup>3</sup>), an increase in pressure by an order of magnitude, from 5 to 50 bar ( $\times$  and  $\diamond$ ), results in only half the soot yield.

### Discussion

For the three hydrocarbons, ethylene, *n*-hexane, and benzene, soot formation behind reflected shock waves has been investigated in order to check the influence of pressure on soot formation in pyrolysis. Optical measurements have been performed to determine soot yields, and gas samples have been analyzed to obtain information about gaseous growth species. Soot samples were examined by electron microscopy to measure average particle diameters.

In general, the three substances investigated behave differently regarding soot formation, the strongest difference being between aromatic and nonaromatic fuels. No pressure dependence of the induction times and of the formal rates of soot growth, normalized by carbon concentration, was found. The data for ethylene and *n*-hexane agree quantitatively fairly well, whereas benzene shows induction times that are shorter and rate constants that are larger by about an order of magnitude than those of the nonaromatics for equal C-atom concentrations.

A main part of that difference is due to processes in the pyrolysis of the different hydrocarbons. For *n*-hexane, very early in the reaction methane is formed, which is not readily available for the formation of higher hydrocarbons. For soot formation from alkanes and alkenes, first acetylene has to be formed from which later polycyclic aromatics result. That works more readily from ethylene than from *n*-hexane so that also the formation of polycyclic aromatics, especially towards higher pressures, is favoured, as can be seen from the increase of the soot yield of ethylene with pressure. It is to be expected that the number density of initially formed soot particles is higher for ethylene than for *n*-hexane and still higher for benzene. During benzene pyrolysis, acetylenes and polycyclic aromatics are formed, which favours soot growth in any phase.

As described above, the results of the gas analysis show a complementary behaviour of the gaseous end product curves to the soot yield curves. The main hydrocarbons found are CH<sub>4</sub> and C<sub>2</sub>H<sub>2</sub>, and the concentrations of the latter are much higher than in comparable high-pressure flat flames. The argument made for high-pressure flat flames that soot growth stops because of lack of gaseous growth species seems, therefore, not to be valid for shock-tube conditions.

For *n*-hexane, the derived soot yield curves are very similar at different pressures, and soot yields are low compared to benzene. If one compares the soot yields of hexane and ethylene, the experiments with ethylene at 25 bar gives similar amounts of soot as hexane at all pressures used here. The soot yield in experiments with ethylene is pressure dependent, and at higher pressures, it is higher than that in hexane pyrolysis. The ethylene pyrolysis at 100 bar results in similar soot yields as benzene pyrolysis at 50 bar.

Frenklach et al. [8] reported a pressure effect in toluene pyrolysis. The maximum of the soot yield curve is shifted 300 K in temperature and without changing the value of this maximum. Our results for benzene pyrolysis show a decrease in soot yield with increasing pressure in the range of 5 bar to 50 bar at lower C-atom concentration ( $[C] \approx 2 \cdot 10^{17}$ /cm<sup>3</sup>), but no temperature shift of the soot yield curve has been observed.

The term  $k_f$  depends on total carbon concentration, as can be seen in Fig. 3. In premixed flames, most of the initial carbon is oxidized to CO and CO<sub>2</sub>. An estimation of carbon still available for soot formation behind the oxidation zone can be made from gas analysis results. Here, too, the main hydrocarbons found are C<sub>2</sub>H<sub>2</sub> and CH<sub>4</sub> [21]. The latter is mainly formed in the oxidation zone and is known to play only a minor role in soot formation. An "effective" carbon concentration can, therefore, be calculated as  $[C]_{\text{eff}} = [C]_{\text{tot}} - [CO_2] - [CO] - [CH_4]$ , with values of  $2 \cdot 10^{17}$  to  $8 \cdot 10^{17}$  C atoms/cm<sup>3</sup>, about the same order of magnitude as in shock-tube pyrolysis. In Fig. 3, the soot growth rate constants  $k_f$ , normalized by carbon density, for soot formation from ethylene under shock-tube and flat-flame conditions are plotted. For the shock-tube data, the total C-atom concentration has been used; for the flat-flame data, an "effective" carbon concentration was calculated in the manner described above. The data for pyrolysis and the flat flame are very similar, indicating that the different chemical environments have little influence on  $k_f$ .

Using the optically determined final soot volume fraction and the here-obtained average particle diameters of 20–30 nm, final particle number densities can be calculated, assuming  $N = f_v/\bar{v}$  ( $\bar{v}$  = mean particle volume) and spherical particles. For an average diameter of 25 nm,  $\bar{v}$  is approximately  $10^{-17}$  cm<sup>3</sup>. For the 50-bar benzene experiments with a carbon density of  $2 \cdot 10^{17}$ /cm<sup>3</sup>, an  $f_{v,\infty}$  value of  $5 \cdot 10^{-7}$  was found, which gives an  $N_\infty$  of  $5 \cdot 10^{10}$ /cm<sup>3</sup>. For the experiments with a carbon density larger by two orders of magnitude, similar diameters, but larger soot volume fractions of about  $f_{v,\infty} \approx 10^{-4}$ , were determined, giving an  $N_\infty$  of  $10^{13}$ /cm<sup>3</sup>. For atmospheric pressure premixed flames, number densities of  $10^9$  to  $10^{10}$ /cm<sup>3</sup> are typically found [2], whereas for 70-

bar premixed ethylene-air flames, a number density of  $10^{12}/\text{cm}^3$  was obtained [22].

The primary particles are formed by surface growth and coagulation. The latter process can be described by the Smoluchowski equation:

$$\frac{dN}{dt} = -k_{\text{coag}} \cdot [N]^2 \quad (3)$$

$$\tau_{\text{coag}} = (k_{\text{coag,theo}} \cdot N_{\infty})^{-1}$$

which leads to a characteristic half-life of coagulation  $\tau_{\text{coag}}$  of the particles. Using the particle diameters determined by electron microscopy, Knudsen numbers can be calculated for the investigated temperatures and pressures. They are of the order of 0.1 to 1, and therefore, our experimental conditions are in the transition region from the slip flow regime to continuum [23]. In this region, calculated theoretical values of the coagulation rate constant are of the order of  $5 \cdot 10^{-10} \text{ cm}^3/\text{s}$ . For the benzene experiments with low-carbon densities, a final particle number density,  $N_{\infty} = 5 \cdot 10^{19}/\text{cm}^3$ , results in a half-life of 40 ms. This is too long to see coagulation in our experiments. For the high-carbon densities employed,  $N_{\infty} = 10^{13}/\text{cm}^3$ , giving coagulation half-lives of only 0.2 ms, well within the observation timescale of the shock-tube measurements. Therefore, one would expect different final particle diameters, depending on the characteristic times for coagulation, or rather stable agglomerates.

### Conclusion

The difference in behaviour regarding soot formation between aromatic and nonaromatic fuels could be confirmed in this study for high pressures and carbon concentrations. *n*-hexane shows only low soot yields, even at high pressure, with small  $k_f$  values and long induction times. Benzene shows the highest propensity to soot, with short induction times, large  $k_f$  values, and a slight decrease in soot yield from low to medium pressure. Ethylene behaves basically like a nonaromatic fuel, with values for  $\tau$  and  $k_f$  similar to hexane. But with increasing pressure, increasing soot yields are found, indicating a change in behaviour towards aromatic fuels. Despite these differences between the fuels, average particle diameters, obtained by electron microscopy of soot samples, are very similar under all experimental conditions employed. The data can be described by a narrow log-normal size distribution, with average diameters of 20–30 nm. The different amounts of soot are, therefore, essentially determined by number densities. Furthermore, the results show that at higher pressures, the “meet and stick” coagulation model cannot be applied any more. The gas analysis shows that a lack of acetylene cannot be responsible for the

end of coagulation and soot growth, as observed in high-pressure ethylene-air flames.

### REFERENCES

1. Wagner, H. Gg., *Seventeenth Symposium (International) on Combustion*, The Combustion Institute, Pittsburgh, 1979, p. 3.
2. Haynes, B. S., and Wagner, H. Gg., *Prog. Energy Combust. Sci.* 7:229 (1981).
3. Lahaye, J., and Prado, G., *Soot in Combustion Systems and its Toxic Properties*, Plenum Press, New York, 1983.
4. Wagner, H. Gg., AGARD Report No. 422, Nato, 1988, p. 24–1.
5. Glassman, I., *Twenty-Second Symposium (International) on Combustion*, The Combustion Institute, Pittsburgh, 1988, p. 295.
6. Graham, S. C., Homer, J. B., and Rosenfeld, J. L., *Proc. R. Soc. London A* 344:259 (1975).
7. Wang, T. S., Matula, R. A., and Farmer, R. C., *Eighteenth Symposium (International) on Combustion*, The Combustion Institute, Pittsburgh, 1981, p. 1149.
8. Frenklach, M., Taki, S., and Matula, R. A., *Combust. Flame* 49:275 (1983); Frenklach, M., Taki, S., Durgaprasad, M. B., and Matula, R. A., *ibid.* 54:81 (1983); Frenklach, M., Ramachandra, M. K., and Matula, R. A., *Twentieth Symposium (International) on Combustion*, The Combustion Institute, Pittsburgh, 1984, p. 871.
9. Simmons, B., and Williams, A., *Combust. Flame* 71:219 (1988).
10. Geck, C. C., Diploma Thesis, Universität Göttingen, Göttingen, Germany, 1975.
11. Hwang, S. M., Vlasov, P., Wagner, H. Gg., and Wolff, Th., *Z. Phys. Chem. Neue Folge* 137:129 (1991).
12. Greene, E. F., and Toennies, J.P., *Chemische Reaktionen in Stoßwellen* (Translated by H. Gg. Wagner), Dr. Dietrich Steinkopff Verlag, Darmstadt, 1959.
13. Gardiner, W. C., Jr., Walker, B. F., and Wakefield, C. B., in *Shock Waves in Chemistry* (A. Lifshitz, Ed.), Marcel Dekker, New York, 1981.
14. Lee, S. C., and Tien, C. L., *Eighteenth Symposium (International) on Combustion*, The Combustion Institute, Pittsburgh, 1981, p. 1159.
15. Tanke, D., Ph.D. Thesis, Universität Göttingen, Göttingen, Germany, 1994.
16. Haynes, B. S., and Wagner, H. Gg., *Z. Phys. Chem. Neue Folge* 133:201 (1983).
17. Wagner, H. Gg., “Mass Growth of Soot,” in *Soot in Combustion Systems and its Toxic Properties* (J. Lahaye, and G. Prado, Eds.), Plenum Press, New York, 1983.
18. Mätzing, H., and Wagner, H. Gg., *Twenty-First Symposium (International) on Combustion*, The Combustion Institute, Pittsburgh, 1986, p. 1047.

19. Böhm, H., Hesse, D., Jander, H., Lüers, B., Pietscher, J., Wagner, H. Gg., and Weiss, M., *Twenty-Second Symposium (International) on Combustion*, The Combustion Institute, Pittsburgh, 1988, p. 403.
20. Böning, M., Feldermann, Chr., Jander, H., Lers, B., Rudolph, G., and Wagner, H. Gg., *Twenty-Third Symposium (International) on Combustion*, The Combustion Institute, Pittsburgh, 1990, p. 1581.
21. Feldermann, Ch. J., Ph.D. Thesis, Universität Göttingen, Göttingen, Germany, 1992.
22. Böhm, H., Feldermann, Chr., Heidemann, Th., Jander, H., Lüers, B., and Wagner, H. Gg., *Twenty-Fourth Symposium (International) on Combustion*, The Combustion Institute, Pittsburgh, 1992, p. 991.
23. Hidy, G. M., and Brock, J. R., *The Dynamics of Aerocolloidal Systems*, Pergamon Press, New York, 1979.

## COMMENTS

*Esko I. Kauppinen, VTT Aerosol Technology Group, Finland.* I did not get in detail how you sampled particles from the shock tube for analysis in the TEM. How much could you change the structure of agglomerates during the sampling when you reduce the pressure to ambient conditions? It is known that loose agglomerates may break up by flow-induced shear forces. This relates to the conclusion that the sticking coefficient approaches zero at high carbon concentrations.

*Author's Reply.* The EM samples have been obtained from the shock tube end plate, collected on TEM grids, respectively aluminum plates mounted at the wall of the sampling valve, in the sampling flow and in the sampling flask. The diameters of the spherical particles analyzed by TEM and SEM did not differ markedly for the different collecting methods. The agglomerate sizes were different but did not change towards longer residence times anymore (small effective sticking coefficient).

●

*Ömer L. Gülder, National Research Council of Canada, Canada.* Your benzene pyrolysis results show a decrease in soot yield with increasing pressure, from 5 to 50 bar, at a given C-atom concentration, in contrast to the behaviour of ethylene and *n*-hexane. Do you have any explanation for the observed behaviour of benzene, and do you expect similar results for other aromatic hydrocarbons?

*V. Knorre, Moscow Automobile and Road Construction, Technical University, Russia.* 1. Will you comment on the mechanism of soot formation suppression in the case of *n*-hexane and why this mechanism does not work in the case for example of ethylene?

2. What is the mechanism of the decrease in sticking coefficient?

3. Please comment on the minimum in the curve for benzene.

*Author's Reply.* At present, we relate the different soot yields of benzene, ethylene, and *n*-hexane for different pressures mainly to the different concentrations of PAH and acetylenes at the very beginning of soot particle formation. The formation of acetylenes and PAH is more complicated for *n*-hexane than for  $C_2H_4$ . Towards high pressures, the  $C_2H_4$  and the  $C_6H_6$  soot yields become similar, and it could be that the yield for *n*-hexane will also rise towards high pressures. At low pressure, soot formation in benzene proceeds in a way different from that in  $C_2H_4$  as a result of the "early availability of bigger building bricks." Towards elevated pressure, the concentration of small radicals, which are necessary for the formation of acetylenes and higher PAH and initial soot particles, decreases thus reducing benzene soot yield in a certain pressure range for low carbon atom densities. For carbon atom densities near and above  $10^{18} \text{ cm}^{-3}$ , the effect disappears. Measurements that should help to clarify the situation are underway.

The decrease of the sticking coefficients for larger particles seems to be due to the formation of carbon layers at the particle surface similar to carbon planes in graphite. The particles do not merge any more, and the "glue between the particles"—due to surface growth—becomes much less active so that the sticking is based on van-der-Waals forces.

●

*P. A. Tesner, All Russian Scientific Research Institute, Russia.* The interesting experimental results you obtained during shock tube pyrolysis are different from our results obtained from atmospheric pressure pyrolysis. Meanwhile, our experimental results are in good agreement with those obtained during flat flame combustion conducted at different pressures.